Gelation of Poly(vinyl alcohol)–Vanadate Aqueous Solutions

Mitsuhiro Shibayama,* Masayuki Adachi, Fumiyoshi Ikkai, Hidenobu Kurokawa, Shinichi Sakurai, and Shunji Nomura

Department of Polymer Science and Engineering, Kyoto Institute of Technology, Matsugasaki, Sakyo-ku, Kyoto 606, Japan

Received June 9, 1992; Revised Manuscript Received September 11, 1992

ABSTRACT: The gelation mechanism of poly(vinyl alcohol) (PVA) aqueous solutions in the presence of vanadate ions was studied from the rheological and spectroscopic points of view. A phase diagram of PVA and vanadate ions was constructed as a function of PVA and sodium vanadate concentrations as well as pH. It was found that PVA aqueous solutions became a gel in the presence of $H_2V_{10}O_{28}{}^{4-}$ vanadate ions, which are exclusively formed in the pH range 2–3. Furthermore, ultraviolet (UV) absorption spectra of these solutions indicate that only $H_2V_{10}O_{28}{}^{4-}$ ions among more than 10 kinds of vanadate ions were responsible for the complex formation with PVA molecules. This observation was in good agreement with the phase behavior. The viscosity of PVA solutions containing vanadate ions was measured for several PVA concentrations below and above the so-called C^* concentration, i.e., the chain overlap concentration. The viscosity increased with time when C was larger than C^*. On the other hand, the viscosity decreased for $C < C^*$. The time evolution of the viscosity and UV spectra was also studied. It was found that PVA solutions having only $H_2V_{10}O_{28}{}^{4-}$ ions had a significant time dependence in the viscosity and UV absorption behavior. These facts were successfully explained by the concepts of inter- and intra-cross-linking formations and time-dependent hydrogen-bonding formation.

1. Introduction

Poly(vinyl alcohol) (PVA) has several unique features: it is water soluble, crystallizable, and capable of hydrogen bonding.[1] These characteristic features have made PVA useful for many industrial applications: PVA is used in the production of high-strength fibers,[2] as a viscosity-adjusting reagent in aqueous solutions, in formulating adhesives, and so on. Recently, the gelation capability of PVA has been focused on by many researchers so as to understand the gelation mechanism[3–8] and to develop high-strength fibers,[9] a variety of medical substituents,[10,11] and chemomechanical actuators.[12]

PVA gels are formed by cross-linking formation in terms of either hydrogen bonding followed by crystallization of PVA chains or complexation with several kinds of inorganic ions such as cupric,[13] borate,[14] titanate,[15] and vanadate ions.[16] PVA–borate complexes have been used for preparation of high-strength PVA fibers,[9] where pH or thermoreversible gelation of PVA in the presence of borate ions played an essential role in memorizing the topology of the PVA chains in the extruding process. Recently, these complexes have been studied extensively so as to elucidate the complexation mechanism,[4,5,7,8] the rheological behavior,[3,17,18] and the microscopic structures of these polyion complexes.[19–21] We have been focusing on the complex of PVA–borate ions and have (1) studied the mechanism of gelation by ^{11}B-NMR,[5] (2) proposed a universal relationship among the sol–gel transition temperature, the concentration and degree of polymerization of PVA, the boric acid concentration, and the pH,[6] and (3) observed the microscopic structures of PVA gels and sols by small-angle neutron scattering.[20,21]

In the case of PVA–vanadate ion complexes, the gelation mechanism is rather complicated because the orthovanadate ion in aqueous media undergoes complex hydrolysis–polymerization reactions upon neutralization with acids and produces ions such as $V_2O_7{}^{4-}$, $HV_2O_7{}^{3-}$, $V_{10}O_{28}{}^{6-}$, $HV_{10}O_{28}{}^{5-}$, $H_2V_{10}O_{28}{}^{4-}$, $V_4O_{12}{}^{4-}$, $V_3O_9{}^{3-}$, etc.[22,23] Kawakami et al.[16] reported the capability of gelation between PVA and vanadate ions in an acidic condition. They indicated that highly hot-water-resistant fibers could be produced from PVA–vanadate ion complexes. Although one or some of these ions are responsible for gelation of PVA, the mechanism of complexation and the assignment of the species responsible for the complexation of PVA–vanadate ions have not so far been elucidated. Vanadate ions form more than 10 kinds of complexes in aqueous solutions depending upon the vanadate concentration and pH.[22,23] The structures of these vanadate ions both in crystals[24,25] and in solutions[26–31] have been studied. However, the location of protonation is not yet clear.[30,31]

Studies on the complexation between PVA and vanadate ions can not only elucidate the mechanism of gelation of PVA but also provide another aspect of the vanadate complexes in aqueous systems since the viscosity of the polymer solutions is sensitive to complexation. In addition, ultraviolet (UV) spectroscopy can be applied to investigate the gelation mechanism in this particular case because of strong UV absorption by vanadate ions. Taking advantage of these facts, we performed a series of experiments on PVA–vanadate ions in aqueous solutions and obtained a self-consistent result among the viscosity, phase diagram, and UV spectra from both the thermodynamic and kinetic points of view.

2. Experimental Section

2.1. Sample Preparation. Poly(vinyl alcohol) (PVA) having a number-average degree of polymerization of ca. 1700 was kindly supplied by Unitika Chemical Co. Ltd., Japan. The degree of saponification of the PVA is 99.7 mol %. PVA was dissolved in distilled water and mixed with a prescribed amount of $NaVO_3$ aqueous solution. pH was controlled by adding an aqueous solution of H_2SO_4. The pH of the sample solutions was measured with an L-7LC pH meter (Horiba Seisakusho Co., Ltd.).

2.2. Sol–Gel Transition Curve and Phase Diagram. The sol–gel transition curve as well as phase diagram of the PVA–vanadate ion complex was determined by the "test-tube tilting" procedure: The solution was kept in a 10-mm-thick test tube in a dark room for a given time at 25 °C and its flow behavior checked by tilting the test tube. If the contents of the test tube did not flow when the tube was held upside down, we decided that the solution was gelled. The phase behavior was determined by visual observation. Note that vanadate ions are sensitive to

---

* To whom correspondence should be addressed.

0024-9297/93/2226-0623$04.00/0

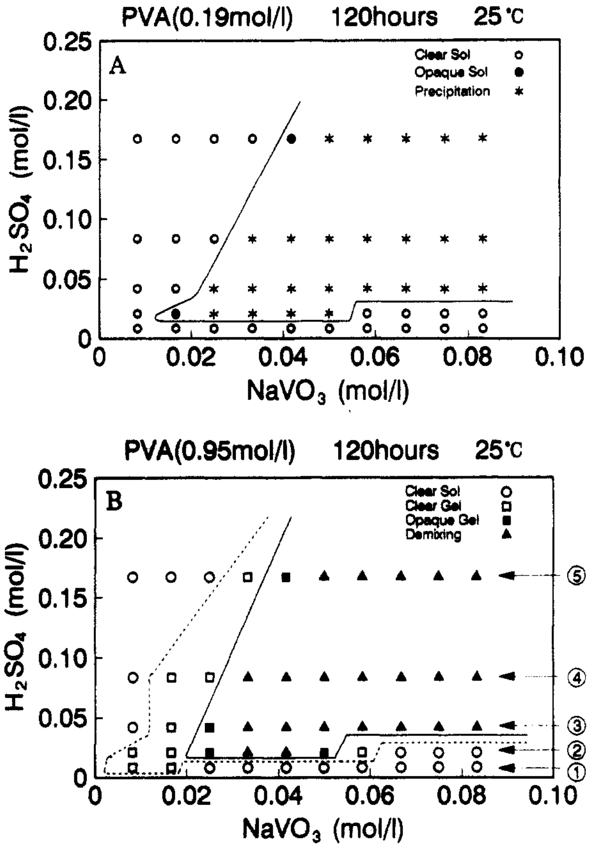

Figure 1. Phase diagrams of PVA–vanadate aqueous solutions at 25 °C determined 120 h after preparation: (A) $C = 0.19$ mol/L; (B) 0.95 mol/L. The solid and dashed lines indicate the clear–opaque transition and the sol–gel transition lines, respectively. Numbers in B indicate the trajectories of the pH dependence experiment which is discussed in relation to Figure 2.

light. When this procedure was conducted in a bright room, the color of the solution gradually turned to blue or green, indicating that the valence of the vanadium atom changed from 5 to 4, i.e., V^V to V^{IV}.

2.3. Ultraviolet Absorption Spectroscopy. Ultraviolet absorption spectroscopy was conducted with a UV-160 ultraviolet (UV) photometer (Shimadzu Seisakusho Co., Ltd.). The range of wavelength observation was from 200 to 600 nm. A quartz cell having a 1-mm optical path was used as a sample container. Because of the difficulty in handling the gel samples, all spectroscopic measurements were made for samples in a sol state. No significant change in the spectrum during the experiment due to the irradiation of UV light was detected.

2.4. Viscometry. The viscosity of the PVA–vanadate solutions was measured with a Ubbelohde capillary viscometer at 25 ± 0.5 °C.

3. Results and Discussion

3.1. Phase Behavior. Figure 1 shows the phase diagrams of PVA aqueous solutions of $C = 0.19$ mol/L (Figure 1A) and 0.95 mol/L (Figure 1B). The ordinate and abscissa are the concentrations of H_2SO_4 and $NaVO_3$, respectively. The system was yellow throughout the concentration range of observation, which was due to the presence of vanadate ions of type V^V. The solid and dashed lines in the figures represent the clear–opaque transition line and the sol–gel transition line, respectively. Open circles, closed circles, open squares, closed squares, closed triangles, and asterisks indicate, respectively, clear sol, opaque sol, clear gel, opaque gel, demixing, and precipitation as shown in the figures. Demixing means a phase-separated state due to deswelling of gels, whereas precipitation indicates an aggregation of PVA in the sol state (or solution). All of the samples shown here were clear when they were prepared. However, upon aging, some of the samples underwent changes of state from a clear sol to the states indicated with these symbols. These significant changes of state occurred within 24 h, and no further change was observed after 120 h. Therefore it was assumed here that all of the samples reached a thermodynamic equilibrium within 120 h. The numbers from 1 to 5 in Figure 1B indicate the trajectories of the pH dependence experiment, which will be discussed in relation to Figure 2.

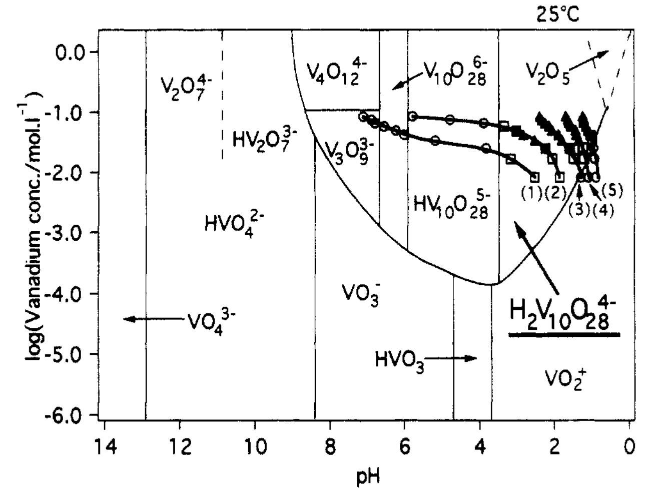

Figure 2. Diagram of states of vanadate ions reported by Schiller et al.[22] The ordinate is the logarithm of the vanadium concentration. The thick solid lines marked as 1–5 and with symbols indicate the paths of the $NaVO_3$ concentration dependence of the phase behavior of PVA–vanadate aqueous solution. The meanings of the symbols are the same as those in Figure 1.

It is noteworthy that a gel phase is observed for a system having the PVA concentration ($C = 0.95$ mol/L but not for a system having $C = 0.19$ mol/L. This is due to the fact that the so-called C^* concentration, the polymer concentration at which the polymer chains start to overlap, is between these concentrations. For PVA solutions at $C < C^*$, a precipitation is expected by introducing cross-linking formation. On the other hand, a phase demixing is observed for PVA solutions at $C > C^*$ due to a phase separation between polymer-rich and polymer-poor phases.

Figure 2 shows the diagram of states of vanadate ions in aqueous solution reported by Schiller et al.[22] (hereafter we call this the Shiller–Thilo phase diagram). The ordinate is the logarithm of the vanadium concentration. As shown in the figure, there are more than 10 different species of vanadate ions. The thick solid curves marked 1–5 indicate the paths of the experiment for the $NaVO_3$ concentration dependence of the phase behavior of the PVA–vanadate aqueous solution as shown in Figure 1B. The symbols on the curves are also the same as those in Figure 1B. This Shiller–Thilo phase diagram was observed by changing the concentration of $NaVO_3$ at constant H_2SO_4. During this experiment, the pH of the system was also measured. Curves 1–5 clearly indicate that $H_2V_{10}O_{28}{}^{4-}$ ions are exclusively responsible for the gelation of PVA.

Since an aqueous solution of vanadate ions absorbs yellow to ultraviolet light, we explore the mechanism of PVA–vanadate complexation in terms of UV–visible light spectroscopy in the following section.

3.2. UV Spectroscopy. Figure 3 shows the UV absorption spectra of $NaVO_3$ aqueous solutions with (dashed line) and without PVA (solid line). The $NaVO_3$ concentration was fixed at 4×10^{-3} mol/L. The concentration of PVA was 0.57 mol/L for the case of $NaVO_3$ solution with PVA. The species of vanadate ions varied

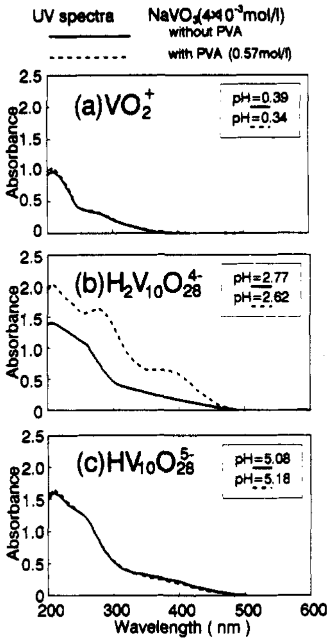

Figure 3. UV-visible light spectra for $NaVO_3$ aqueous solutions with (dashed line) and without PVA (solid line). The $NaVO_3$ concentration was fixed at 4×10^{-3} mol/L. The concentration of PVA was 0.57 mol/L for the case of the $NaVO_3$ solution with PVA.

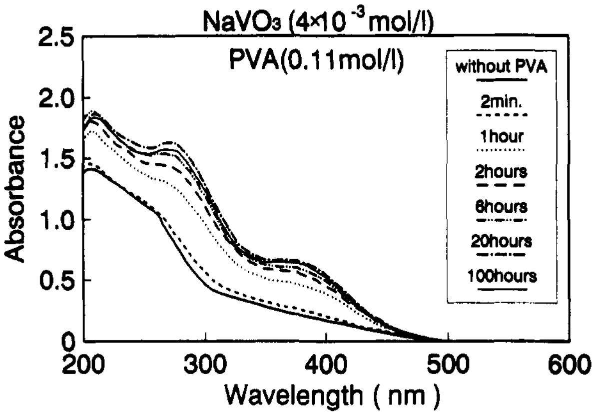

Figure 4. Time evolution of the UV spectra for a solution of C = 0.11 mol/L and pH 2.85.

systematically by changing pH. In the case of Figure 3a, VO_2^+ ions are expected in the solution because the pH is around 0.3–0.4, i.e., a very highly acidic condition. In this case, no significant difference was observed between the spectra of $NaVO_3$ solutions with and without PVA. When pH increases to ca. 2.7, $H_2V_{10}O_{28}^{4-}$ ions become dominant in the system. In this case, a distinct difference between the spectra of the solutions with and without PVA was detected as shown in Figure 3b. A $NaVO_3$ solution containing PVA has a higher absorption over the entire range of observation wavelengths. In addition, distinct maxima in the absorption were detected around 207, 275, and 375 nm. When pH further increases to over 5, $HV_{10}O_{28}^{5-}$ ions become dominant in the system. In this case, however, no difference in the absorption spectra form the solutions with and without PVA was detected. According to UV absorption spectroscopy, $H_2V_{10}O_{28}^{4-}$ ions react exclusively with PVA molecules, which is in good accordance with the observation of gelation.

Figure 4 shows the time evolution of the UV spectra for a solution of C = 0.11 mol/L and pH 2.85. In this condition, $H_2V_{10}O_{28}^{4-}$ ions are again expected in the system. The absorption increases with time and is saturated in about 6 h after sample preparation. This time evolution of the absorption spectrum indicates that a time-dependent complexation occurs in the system. Taking into account the fact that PVA molecules in an aqueous solution are capable of crystallization due to hydrogen bonding, PVA crystallization and/or a hydrogen-bonding reaction might occur cooperatively in addition to the complexation between PVA and $H_2V_{10}O_{28}^{4-}$ ions. This type of time dependence was not observed in the PVA–borate system.[18] It is known for polyions, such as poly(acrylic acid), that a basic condition reduces the capability of hydrogen bonding compared to neutral or acidic conditions.[32] A similar phenomenon was observed in PVA aqueous solutions.[33] Therefore the time dependence of gelation or complexation of PVA–vanadate ions might be due to a complexation-induced hydrogen bonding formation, which in turn develops the complexation. On the other hand, the PVA–borate ion system is stable with respect to time as discussed in the previous papers.[6,18,21]

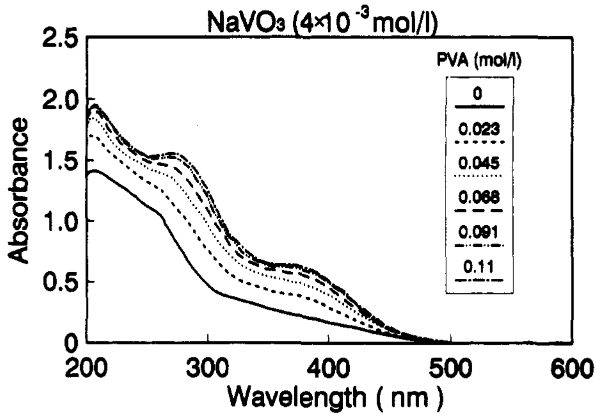

Figure 5. C dependence of UV spectra of $H_2V_{10}O_{28}^{4-}$ ions. The concentration of $NaVO_3$ was 4 mM.

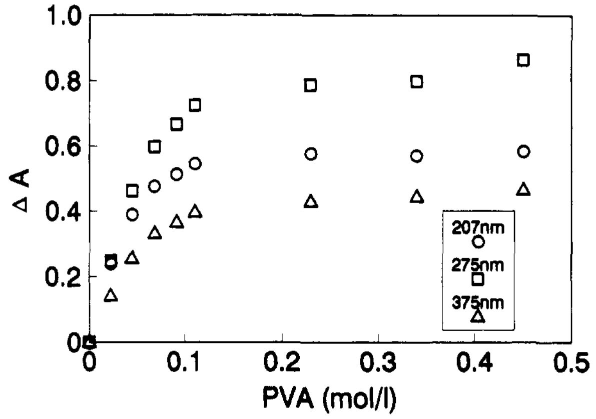

Figure 6. C dependence of the subtracted absorption, ΔA, at 207, 275, and 375 nm.

Figure 5 shows the PVA concentration, C, dependence of the UV absorption spectra. The concentration of $NaVO_3$ was kept at 4 mM. As C increases, the absorption increases and peaks appear at around 207, 275, and 375 nm. Similar phenomena were observed for systems having different $NaVO_3$ concentrations, i.e., 1, 2, 3, and 5 mM.

Figure 6 shows the C dependence of the subtracted absorption, ΔA, at 207, 275, and 375 nm. ΔA was obtained by subtracting the absorption for the PVA-free spectrum from the one with PVA at a given wavelength. This figure indicates that the complexation is saturated at around C = 0.1 M. At this concentration, the molar ratio of $H_2V_{10}O_{28}^{4-}$ ions and PVA monomers is 1/300. Therefore each PVA chain, having a degree of polymerization of 1700, stoichiometrically has about 11 cross-linking points, where we assume that the functionality of the vanadate ion is 2

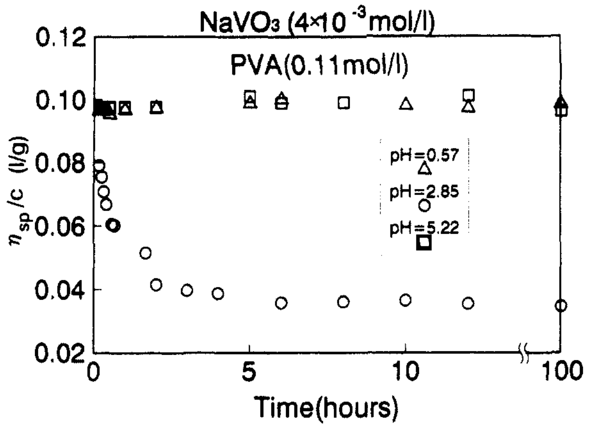

Figure 7. Time evolution of the viscosity number, η_{sp}/C, for PVA–vanadate aqueous solutions at pH 0.57, 2.85, and 5.22.

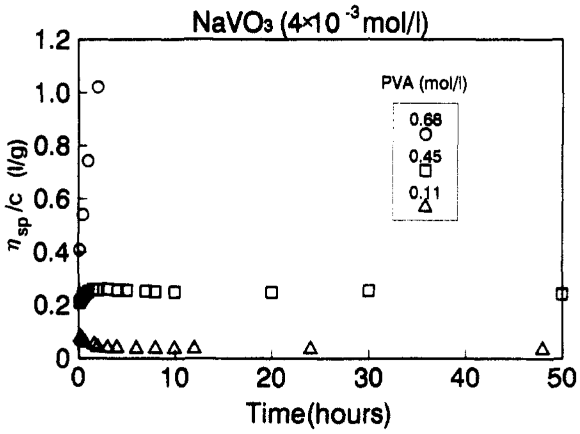

Figure 8. Time dependence of η_{sp}/C for PVA–vanadate aqueous solutions having different PVA concentrations, C = 0.68, 0.45, and 0.11 mol/L.

and that there is complete reaction between vanadate ions and PVA molecules. The reason for this saturation is not yet understood. However, the repulsive Coulombic interaction between tagged vanadate ions on PVA chains could be a negative driving force for the gelation as well as the entropy elasticity of the PVA subchains between cross-links, which contributes to the equilibrium of the complexation.

3.3. Viscometry. Figure 7 shows the time evolution of the viscosity number, η_{sp}/C, for PVA–vanadate aqueous solutions at pH 0.57, 2.85, and 5.22. C is the PVA concentration and η_{sp} is the specific viscosity given by

$$\eta_{sp} = (\eta - \eta_0)/\eta_0 \qquad (1)$$

η and η_0 are the viscosities of the sample solution and of the solvent measured at 25 °C. These pHs were chosen to focus on three kinds of vanadate ions, i.e., VO_2^+, $H_2V_{10}O_{28}^{4-}$, and $HV_{10}O_{28}^{5-}$, respectively, for pH 0.57, 2.85, and 5.22. For the solution at pH 2.85, η_{sp}/C has a strong time dependence. η_{sp}/C decreases steeply with time within a few hours and then reaches a plateau. Contrary to this, the solutions at pH 0.57 and pH 5.22 do not have any time dependence of η_{sp}/C. Although the time dependence of η_{sp}/C was measured up to 100 h after preparation, no further change was detected. This result suggests that only $H_2V_{10}O_{28}^{4-}$ ions take part in the complexation between PVA and vanadate ions, which is in good agreement with the result obtained by UV measurement.

A similar experiment on the time evolution of η_{sp}/C was conducted by changing the PVA concentration. Figure 8 shows the time dependence of η_{sp}/C for PVA–vanadate aqueous solutions having different PVA concentrations at pH 2.85, C = 0.68, 0.45, and 0.11 mol/L. For C = 0.68 mol/L, a steep increase in η_{sp}/C is observed, which is due to intermolecular cross-linking formation. On the other hand, a slight decrease in η_{sp}/C is detected for the solution of C = 0.11 mol/L, which is far below C^*. For C = 0.45 mol/L, η_{sp}/C increases slightly in the beginning and then reaches a plateau. This result strongly indicates the difference in the complexation mechanism, i.e., intermolecular cross-linking formation (C = 0.68 mol/L) and intramolecular cross-linking formation (C = 0.11 mol/L).

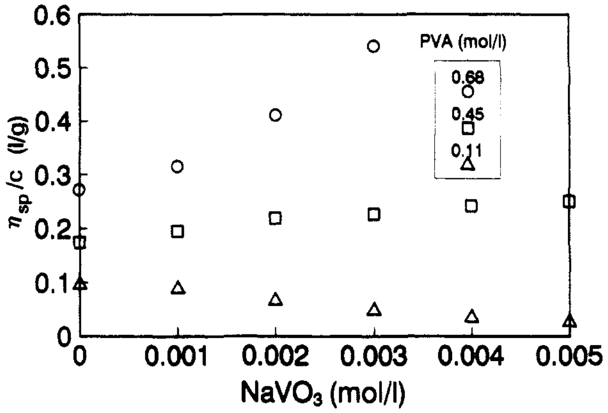

Figure 9. $NaVO_3$ concentration dependence of η_{sp}/C for PVA–vanadate solutions having different PVA concentrations, C = 0.68, 0.45, and 0.11 mol/L. pH was fixed to be around 2.6–2.9 so as to generate $H_2V_{10}O_{28}^{4-}$ ions.

The viscosity number is given by[34]

$$\eta_{sp}/C = [\eta] + k'[\eta]^2C \qquad (2)$$

where $[\eta]$ is the intrinsic viscosity and k' is the Huggins constant. The Huggins constant k' depends on the kind of solvent and temperature and does not depend on the polymer molecular weight. Therefore k' is an invariant in this study. The intrinsic viscosity $[\eta]$ is a measure of the individual polymer dimension since it is proportional to the cube of the hydrodynamic radius of the polymer chains. The decrease in η_{sp}/C is due to the contraction of individual PVA polymer chains, which results from the intramolecular cross-linking formation.

In the case of C = 0.68 mol/L, on the other hand, intermolecular cross-linking takes place as a preliminary stage of gelation since the concentration is much larger than C^*. As a result, η_{sp}/C increases and diverges with time. The behavior of the solution of C = 0.45 mol/L might be the case in between the two extremes. In other words, the contributions of the inter- and intramolecular cross-linking formations to the net size of the polymer chains compensate one another. Regarding the strong concentration dependence of η_{sp}/C, a similar phenomenon was observed by Ochiai[3] and was theoretically explained by Pezron et al.[17] for a PVA–borate aqueous system. We also found in a PVA–borate system that the intrinsic viscosity is very sensitive to the formation of intra- and interchain cross-links, which also affected the phase behavior.[18] The time variation of η_{sp}/C, however, seems to be uniquely observed in this PVA–vanadate aqueous system.

Figure 9 shows the $NaVO_3$ concentration dependence of η_{sp}/C for the PVA–vanadate solutions having different PVA concentrations, C = 0.68, 0.45, and 0.11 M. pH was fixed to be around 2.6–2.9 so as to generate $H_2V_{10}O_{28}^{4-}$ ions. A behavior similar to that of Figure 8 was observed depending on the relative concentrations of C with respect to C^*.

3.4. Structure of the PVA–Vanadate Ions. Figure 10 shows the structure of the polyoxyvanadate ion $V_{10}O_{28}^{6-}$,

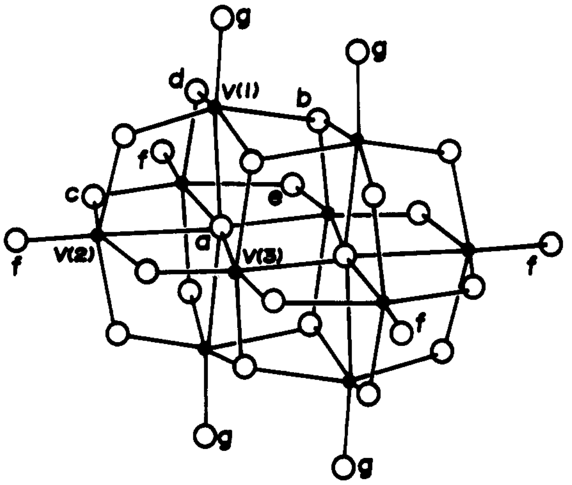

Figure 10. Ionic structure of $V_{10}O_{28}^{6-}$. Small dots and large open circles indicate vanadium and oxygen atoms, respectively. V(1) to V(3) indicate the difference in atomic state of vanadium ions as revealed by ^{51}V-NMR. a–h are oxygen atoms having different environments.

which has been identified in aqueous solutions[26–31] as well as in crystals.[24,25] Small dots and large open circles indicate vanadium and oxygen atoms, respectively. It is known from ^{51}V-NMR that three different states of vanadium atoms are present, which are named V(1), V(2), and V(3).[29,30] According to this fact, seven different states of oxygen atoms are also classified and labeled a–g as shown in the figure.

The structure of $H_2V_{10}O_{28}^{4-}$, which was verified to be in charge of the complex formation, can be obtained by adding two protons next to two of the oxygen atoms in the figure. According to Howarth et al.,[30] protons are located next to the f- or g-oxygen atom (apical oxygen). On the other hand, Klemperer et al.[31] predicted that protons were selectively bonded to b-oxygens (bridge oxygen) by their ^{17}O-NMR experiment. Although the exact structure has not been determined yet, we expect here that protons can be bonded to f-oxygen or g-oxygen (apical) atoms and the rest of the apical oxygens are used for cross-linking formation because of the less steric hindrance, which is quite deterministic, particularly in the case of gel formation. Since there are four f-oxygens and four g-oxygens in a $V_{10}O_{28}^{6-}$ ion, $H_2V_{10}O_{28}^{4-}$ can be a multifunctional cross-linking point with the number of functionality of 2–8, depending on the chemical reactivity of the ion with PVA. Direct assignment of the PVA–vanadate complex has to be carried out out by a more direct analytical method, such as ^{51}V-NMR, in the presence of PVA as was done by ^{11}B-NMR for the case of PVA–borate complexes.[5]

4. Conclusions

PVA–vanadate ion complexation was studied by the observation of the sol–gel transition and phase separation behavior, viscosity measurement, and UV absorption spetroscopy. It was found that $H_2V_{10}O_{28}^{4-}$ ions are exclusively responsible for the complexation with PVA molecules owing to the quantitative comparison of the sol–gel transition behavior and the Shiller–Thilo diagram for vanadate ions. Only $H_2V_{10}O_{28}^{4-}$ ions, which were formed at pH 2–3, showed a significant variation in the UV absorption spectrum by introducing PVA molecules into the system. Three distinct peaks in the absorption spectra appeared at 207, 275, and 375 nm in a PVA-vanadate solution in the presence of $H_2V_{10}O_{28}^{4-}$ ions and PVA. This complexation leads to a precipitation of PVA molecules when C is lower than C^*. On the other hand, a gelation occurs for $C > C^*$. The difference in these behaviors results from the difference in the complexations, intra- and intermolecular cross-linking formations. The difference in the complexations was clearly observed by time evolution of the viscosity number as well as UV absorption at the characteristic wavelengths. The time evolution is due to the cooperative phenomenon of the hydrogen bond formation and PVA–vanadate complexation.

Acknowledgment. The authors are grateful to Dr. Q. Tran-Cong for discussion and kindly making available of the UV photometer.

References and Notes

(1) Sakurada, I. *Polyvinyl alcohol* (Japanese Edition); The Society of Polymer Science: Tokyo, 1955.
(2) Sakurada, I. *Polyvinyl Alcohol Fibers*; Marcel Dekker: New York, 1985.
(3) Ochiai, H.; Kurita, Y.; Murakami, I. *Makromol. Chem.* **1984**, *185*, 167.
(4) Sinton, S. *Macromolecules* **1987**, *20*, 2430.
(5) Shibayama, M.; Sato, M.; Kimura, Y.; Fujiwara, H.; Nomura, S. *Polymer* **1988**, *29*, 336.
(6) Shibayama, M.; Yoshizawa, H.; Kurokawa, H.; Fujiwara, H.; Nomura, S. *Polymer* **1988**, *29*, 336.
(7) Pezron, E.; Ricard, A.; Lafuma, F.; Audebert, R. *Macromolecules* **1988**, *21*, 1126.
(8) Pezron, E.; Leibler, L.; Ricard, A.; Lafuma, F.; Audebert, R. *Macromolecules* **1989**, *22*, 1169.
(9) Fujiwara, H.; Shibayama, M.; Chen, J.; Nomura, S. *J. Appl. Polym. Sci.*, **1989**, *37*, 1403.
(10) Yamauchi, A. In *Polymer Gels*; DeRossi, D., et al., Eds.; Plenum Press: New York, 1991; p 127.
(11) Ichijo, H.; Ichimura, K.; Uedaira, H.; Suehiro, T.; Nagasawa, J.; Yamauchi, A.; Aisaka, N. In ref 10, p 135.
(12) Suzuki, M. In ref 10, p 221.
(13) Saito, S.; Okuyama, H. *Kolloid Z.* **1954**, *139*, 150.
(14) Deuel, H.; Neukom, A. *Makromol. Chem.* **1949**, *3*, 113.
(15) Crisp, J. D. US Patent 258193, 1946.
(16) Kawakami, H.; Fujiwara, H.; Kinoshita, Y. Jpn Patent S47-40894, 1972.
(17) Leibler, L.; Pezron, E.; Pincus, P. A. *Polymer* **1988**, *29*, 1105.
(18) Kurokawa, H.; Shibayama, M.; Ishimaru, T.; Wu, W.; Nomura, S. *Polymer* **1992**, *33*, 2182.
(19) Wu, W.; Shibayama, M.; Roy, S. K.; Kurokawa, H.; Coyne, R. D.; Nomura, S.; Stein, R. S. *Macromolecules* **1990**, *23*, 2245.
(20) Kajiwara, K.; Kohjiya, S.; Shibayama, M.; Urakawa, H. In *Polymer Gels*; DeRossi, D., et al., Eds.; Plenum Press: New York, 1991; p 3.
(21) Shibayama, M.; Kurokawa, H.; Nomura, S.; Muthukumar, M.; Stein, R. S.; Roy, S. K. *Polymer* **1992**, *33*, 2883.
(22) Schiller, K.; Thilo, E. *Anorg. Z. Anorg. Allg. Chem.* **1961**, *261*, 310.
(23) Murmann, K.; Giese, K. C. *Inorg. Chem.* **1978**, *17*, 1160.
(24) Swallow, A. G.; Ahmed, F R.; Barnes, W. H. *Acta Crystallogr.* **1966**, *21*, 397.
(25) Evans, H. T., Jr. *Inorg. Chem.* **1966**, *5*, 967.
(26) Howarth, O. W.; Richards, R. E. *J. Chem. Soc.* **1965**, 864.
(27) Hatton, J. W.; Saito, Y.; Schneider, W. G. *Can. J. Chem.* **1965**, *43*, 47.
(28) Kazanskii, L. P.; Spitsyn, V. I.; Dokl. Akad. Nauk. *SSSR* **1975**, *223*, 1798.
(29) O'Donnel, S. E.; Pope, M. T., *J. Chem. Soc., Dalton Trans.* **1976**, 2290.
(30) Howarth, O. W.; Jarrold, M. *J. Chem. Soc., Dalton Trans.* **1978**, 503.
(31) Klemperer, W. G.; Shum, W. *J. Am. Chem. Soc.* **1977**, *99*, 3544.
(32) Annaka, M.; Tanaka, T. *Nature* **1992**, *355*, 430.
(33) Ishimaru, T.; Shibayama, M., unpublished results.
(34) Flory, P. J. *Principles of Polymer Chemistry*; Cornell University Press: Ithaca, NY, 1953.